RSC Advances

PAPER

View Article Online
View Journal | View Issue

Cite this: *RSC Adv.*, 2020, **10**, 29129

Supramolecular organogels fabricated with dicarboxylic acids and primary alkyl amines: controllable self-assembled structures†

Lieqiang Liao, ‡[ab] Xiang Zhong, ‡[b] Xinjian Jia, [b] Caiyun Liao, [b] Jinlian Zhong, [b] Shunmin Ding, [a] Chao Chen, *[a] Sanguo Hong*[a] and Xuzhong Luo *[b]

Supramolecular organogels are soft materials comprised of low-molecular-mass organic gelators (LMOGs) and organic liquids. Owning to their unique supramolecular structures and potential applications, LMOGs have attracted wide attention from chemists and biochemists. A new "superorganogel" system based on dicarboxylic acids and primary alkyl amines ($R-NH_2$) from the formation of organogels is achieved in various organic media including strong and weak polar solvents. The gelation properties of these gelators strongly rely on the molecular structure. Their aggregation morphology in the as-obtained organogels can be controlled by the solvent polarity and the tail chain length of $R-NH_2$. Interestingly, flower-like self-assemblies can be obtained in organic solvents with medium polarity, such as tetrahydrofuran, pyridine and dichloromethane, when the gelators possess a suitable length of carbon chain. Moreover, further analyses of Fourier transformation infrared spectroscopy and ^1H nuclear magnetic resonance spectroscopy reveal that the intermolecular acid–base interaction and van der Waals interaction are critical driving forces in the process of organogelation. In addition, this kind of organogel system displays excellent mechanical properties and thermo-reversibility, and its forming mechanism is also proposed.

Received 9th June 2020
Accepted 24th July 2020

DOI: 10.1039/d0ra05072e

rsc.li/rsc-advances

1. Introduction

Since molecularly-ordered states often possess more remarkable optical, chemical and physical properties compared to molecular free states, much endeavor has been made to fabricate functional supramolecular structures *via* self-assembly of small organic molecules. When subjected to special self-assembly conditions, individual molecules can undergo an aggregation process to form various nano/microshapes, such as fibers, tubes, sheet, micelles, vesicles, helixes, hollow spheres *etc.*, displaying fascinating functional properties.[1–7] Although numerous functional supramolecular structures have been reported during the last few decades, the design and preparation of them will continue to be a focus for future research.[8]

As a typical molecularly-ordered state, supramolecular organogels comprised of low-molecular-mass organic gelators (LMOGs) and organic liquids have gained considerable attention due to their rapid development in supramolecular chemistry and potential application in pollutant removal,[9] oil recovery,[10] sensors[11] and catalysis[12] *etc.* They are driven by weak intermolecular non-covalent interactions, such as hydrogen bonds, π–π stacking interactions, electrostatic interactions, van der Waals and hydrophobic interactions. The dynamic and reversible nature of the weak non-covalent interactions endows supramolecular organogels unique ability to create a variety of nano/microstructures with significant characteristics. For example, Hao and co-workers reported a series of serine-based organogelators, which could gel various petroleum products and self-assemble into fibrous nanostructures.[13] Further studies demonstrated that the oils could be separated and collected by acids and distillation, respectively, providing a potential effective treatment of oil-containing water. Liu's group synthesized two enantiomeric L- or D-glutamic acid based lipids at first, and the pure enantiomers could self-assemble into helical nanotubes through organogel formation in ethanol.[14] Subsequently, they designed two types of pyrene-containing gelator molecules. Amazingly, the gelator in which the pyrene group was directly bonded to the glutamide moiety self-assembled into nanotubes in DMSO, the other bearing three methylene spacers only

[a]*Key Laboratory of Jiangxi Province for Environment and Energy Catalysis, College of Chemistry, Nanchang University, Nanchang 330031, P. R. China. E-mail: chaochen@ncu.edu.cn; hongsanguo2020@163.com*

[b]*Key Laboratory of Organo-Pharmaceutical Chemistry of Jiangxi Province, College of Chemistry and Chemical Engineering, Gannan Normal University, Ganzhou 341000, P. R. China. E-mail: luoxuzhong@hotmail.com*

† Electronic supplementary information (ESI) available: The measurement results of gelation property, SEM, DSC, IR, XRD and rheology, Tables S1–S9, and Fig. S1–S6. See DOI: 10.1039/d0ra05072e

‡ These authors contributed equally to this work.

yielded nanorod structures.[15] Kim's team described some stimulus-responsive supramolecular structures in the form of fibers, gels and spheres, derived from an azobenzene-containing benzenetricarboxamide derivative. Their photoinduced, reversible self-assembly process is of great significance in the context of potential applications to supramolecular memory systems.[16] Bag and Dash investigated the gelling properties of betulin in different organic liquids for the

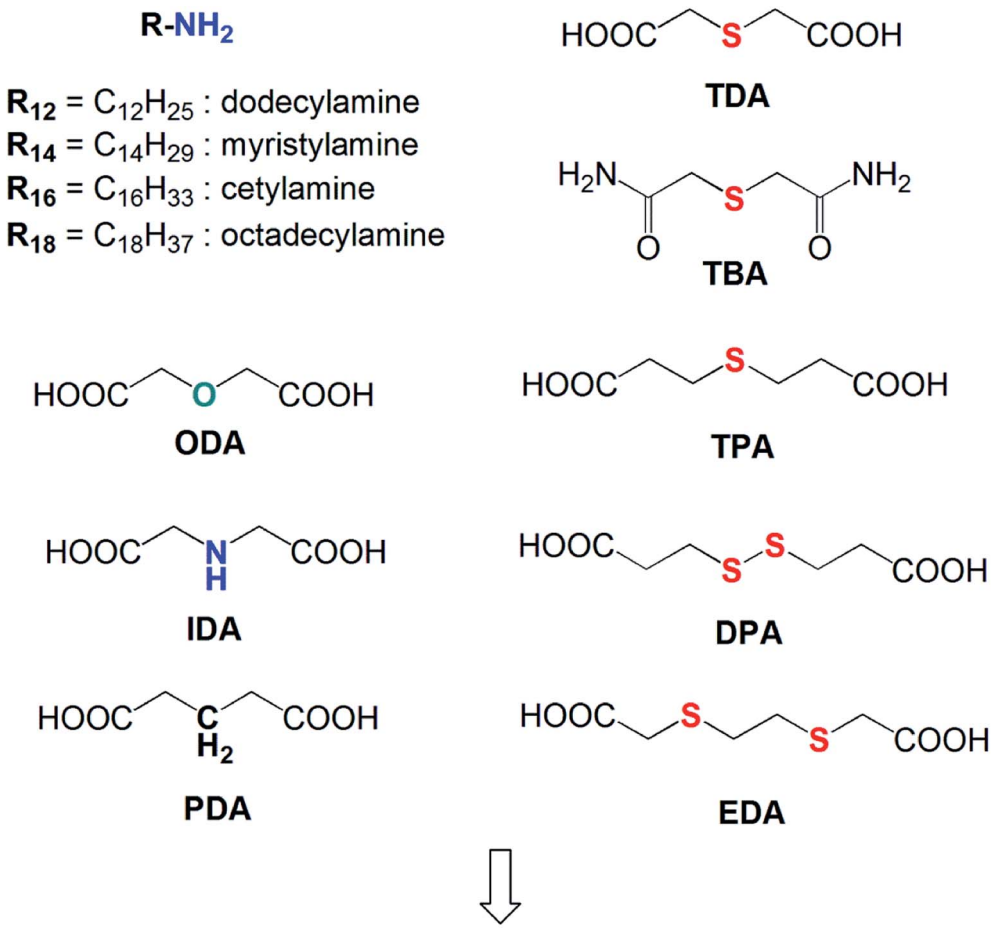

Complexes (Acid:Amine = 1:2)

DPA-R_{12} = DPA + R_{12}	EDA-R_{12} = DPA + R_{12}
DPA-R_{14} = DPA + R_{14}	EDA-R_{14} = DPA + R_{14}
DPA-R_{16} = DPA + R_{16}	EDA-R_{16} = DPA + R_{16}
DPA-R_{18} = DPA + R_{18}	EDA-R_{18} = DPA + R_{18}

TPA-R_{12} = DPA + R_{12}	TBA-R_{12} = DPA + R_{12}	TDA-R_{12} = DPA + R_{12}
TPA-R_{14} = DPA + R_{14}	TBA-R_{14} = DPA + R_{14}	TDA-R_{14} = DPA + R_{14}
TPA-R_{16} = DPA + R_{16}	TBA-R_{16} = DPA + R_{16}	TDA-R_{16} = DPA + R_{16}
TPA-R_{18} = DPA + R_{18}	TBA-R_{18} = DPA + R_{18}	TDA-R_{18} = DPA + R_{18}

PDA-R_{12} = DPA + R_{12}	IDA-R_{12} = DPA + R_{12}	ODA-R_{12} = DPA + R_{12}
PDA-R_{14} = DPA + R_{14}	IDA-R_{14} = DPA + R_{14}	ODA-R_{14} = DPA + R_{14}
PDA-R_{16} = DPA + R_{16}	IDA-R_{16} = DPA + R_{16}	ODA-R_{16} = DPA + R_{16}
PDA-R_{18} = DPA + R_{18}	IDA-R_{18} = DPA + R_{18}	ODA-R_{18} = DPA + R_{18}

Scheme 1 Structures and abbreviations of different acids and alkylamines.

first time, and found that it could self-assemble hierarchically to 3D flower-like architectures of nano to micrometer diameters *via* the formation of fibrillar networks.[17] Moreover, the porous self-assemblies of betulin could be utilized for the entrapment of fluorophores including the anticancer drug doxorubicin and the selective removal of toxic dyes such as rhodamine 6G, crystal violet and methylene blue from aqueous solutions.

In contrast with single-component supramolecular organogels, the controllability of microstructure, aggregation morphology and functionalization for multi-component supramolecular organogels is more complicated.[18] Edwards and Smith reported a two-component acid–amine gelation system based on G2-Lys (a second generation lysine dendron) and monoamines, which could form instant organogels after simple mixing.[19] They noticed that complex formation and nanofiber assembly existed in the hierarchical assembly process, and both steps played a significant role in component selection. Zhang and co-workers described a multi-function two-component organogel system formed from D-gluconic acetal-based derivatives and aliphatic acids, which not only exhibited high-efficiency self-healing with enhanced viscoelasticity and phase selective properties, but also showed potential applications in the fields of flexible optical device fabrication and waste water treatment.[20] Song's team prepared a smart two-

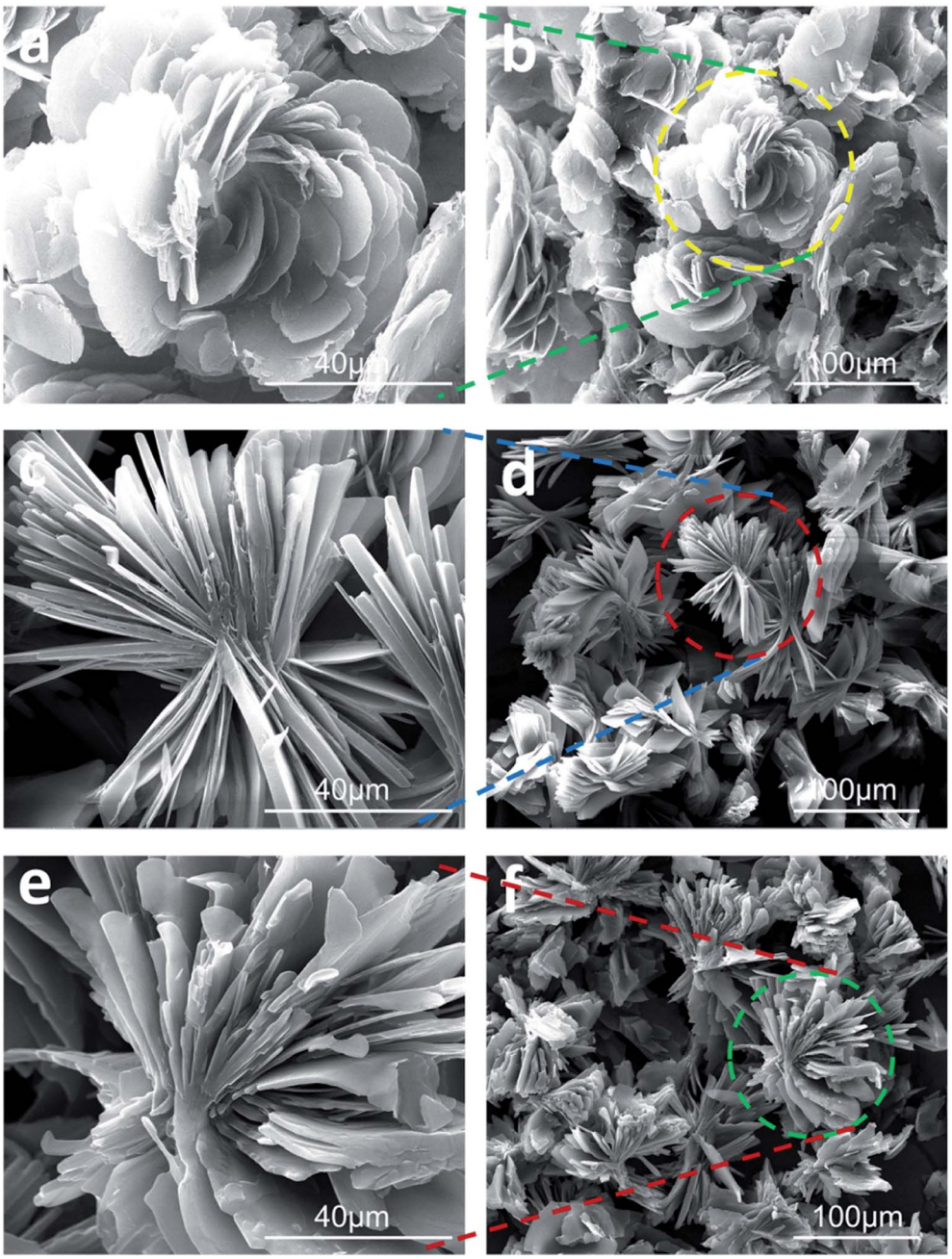

Fig. 1 FE-SEM images of xerogels correlated with (a and b) DPA-R_{18}, (c and d) DPA-R_{16} and (e and f) DPA-R_{14}.

component organogel system by the combination of two gelators based on sorbitol-appended compounds. The obtained supramolecular organogels exhibited intelligent thermochromic properties and had potential application in sensor devices, novel electronic or optical materials, *etc*.[21] Inspired by the excellent achievements, our group previously reported an unprecedented two-component organogel system based on succinamic acid derivatives and primary alkyl amines, which could be utilized for constructing different types of supramolecular organogels, including heat-set gels, conventional gels and irreversible heat-set gels.[22] Although multi-component supramolecular gels with various self-assembly structures and functions have been reported, the controllable preparation is still full of challenges. Therefore, we tried to further enrich the two-component organogel system and investigate its morphology, microstructure and self-assembly mechanism to provide more guidance for designing new functionalized supramolecular self-assembly materials.

In this paper, we present the gelation performance for a new series of two-component gelators based on dicarboxylic acid and primary alkyl amines. The relationship between gelation behavior and molecular structure was then investigated. Moreover, the morphology and microstructure of the corresponding xerogels were also characterized. Thermo-stability and thermo-reversible behavior were further explored. In addition, the mechanical performances of this kind of organogel system were analyzed, and the relevant self-assembly mechanism was finally proposed.

2. Experimental section

2.1 Materials

All organic solvents were obtained from Tianjin Damao Chemical Reagent Factory (Tianjin, China). Analytical grade 2,2′-oxydiacetic acid (ODA), iminodiacetic acid (IDA), 1,5-pentanedioic acid (PDA), 2,2′-thiodiacetic acid (TDA), 2,2′-thiobisacetamide (TBA), 3,3′-thiodipropionic acid (TPA), 3,3′-dithiodipropionic acid (DPA) and 2,2′-(ethylenedithio)diacetic acid (EDA) were purchased from J&K Scientific Co., Ltd. (Shanghai, China). Analytical grade 1-octadecylamine, 1-hexadecylamine, 1-aminotetradecane and 1-dodecylamine were supplied by Adamas Reagent Co., Ltd. (Shanghai, China) and used without further purification.

2.2 Gelation tests

Gelation tests for dicarboxylic acids and alkyl amines (R–NH_2) in organic solutions were investigated by a typical tube inversion method.[3,22] The xerogel was prepared by freeze-drying. The organogel was transferred into a freeze drying vessel (FD-1-50, Beijing BoYiKang Experimental Instrument Co., Ltd.) and dried at −50 °C for 48 h under vacuum condition (<100 Pa) and the xerogel was obtained.

2.3 Characterization

The morphology of xerogels was observed in a field-emission scanning electron microscope (FE-SEM, FEI Quanta 450) coupled with an energy-dispersive X-ray (EDX) detector. The thermo-stability of supramolecular organogels was conducted on a differential scanning calorimeter (DSC, Setaram μDSC7-Evo) at a heating rate of 1.0 °C min^{-1}. Nuclear magnetic resonance (NMR) spectra were acquired by a ^1H NMR spectrometer (Bruker AV400). X-ray powder diffraction (XRD) patterns of xerogels were investigated with a X-ray diffractometer (Bruker D8 Focus) by using the Cu-Kα radiation ($\lambda = 1.5418$ Å). Fourier transform infrared (FT-IR) spectra were recorded with a FT-IR spectrometer (Nicolet Avatar 360) in the 4000 to 400 cm^{-1} region at a resolution of 4 cm^{-1}. The mechanical properties of organogels were performed using a stress-controlled rheometer (HAAKE RheoStress 6000) with parallel plate type geometry (plate diameter, 3.5 cm).

3. Results and discussion

3.1 Gel formation and phase transformation

Organic liquids with various polarities were used for gelation experiments. Gelation tests for the single component of the selected dicarboxylic acids (ODA, IDA, PDA, TDA, TBA, TPA, DPA and EDA) or alkyl amines (R–NH_2, denoted by R_n, $n = 12$, 14, 16 and 18, Scheme 1), as well as the complexes formed from the selected dicarboxylic acids and R–NH_2 were carried out. It has

Table 1 Gelation data of DPA-R_{18}, DPA-R_{16}, DPA-R_{14} and DPA-R_{12} in various organic solvents[a]

Solvents		Complexes (DPA-R_n)			
Name	Polarity	DPA-R_{18}	DPA-R_{16}	DPA-R_{14}	DPA-R_{12}
DMSO	SP	G (1.50)	G (1.98)	G (2.55)	S
Ethylene glycol	SP	G (1.07)	G (3.47)	S	S
Ethanol	SP	G (3.74)	S	S	S
Aminobenzene	SP	G (1.07)	G (6.37)	G (6.93)	S
DMF	SP	G (1.07)	G (1.73)	G (3.19)	S
o-Xylene	MP	G (2.49)	S	S	S
m-Xylene	MP	G (2.49)	S	S	S
Mesitylene	MP	G (2.49)	S	S	S
Nitrobenzene	MP	G (1.67)	G (3.47)	G (6.37)	S
Tetralin	MP	G (3.00)	S	S	S
n-Butyl methacrylate	MP	G (1.00)	G (2.31)	G (2.55)	S
CH_2Cl_2	MP	G (2.49)	G (6.93)	S	S
Pyridine	MP	G (0.94)	G (2.77)	S	S
$CHCl_3$	MP	G (1.67)	G (3.47)	G (4.25)	S
Ethyl acetate	MP	G (1.50)	G (2.31)	G (6.37)	S
o-Dichlorobenzene	MP	G (2.49)	G (2.77)	S	S
Tetrahydrofuran	MP	G (6.37)	G (6.93)	G (7.49)	S
Chlorobenzene	MP	G (2.49)	S	S	S
Aether	MP	G (2.14)	G (2.31)	P	P
Benzene	MP	G (1.87)	S	S	S
Isopropyl ether	MP	G (3.00)	G (3.47)	G (4.25)	S
p-Xylene	MP	G (1.50)	S	S	S
Toluene	MP	G (1.87)	S	S	S
Triethylamine	MP	G (2.14)	G (2.31)	S	S
Cyclohexane	WP	G (1.67)	G (2.31)	G (4.25)	S
Petroleum ether	WP	G (6.37)	G (6.93)	G (7.49)	P

[a] G = gel, S = solution, P = precipitate. The numbers within parentheses represent corresponding MGCs (±0.1%, wt%). SP = strong polarity; MP = medium polarity; WP = weakly polarity.

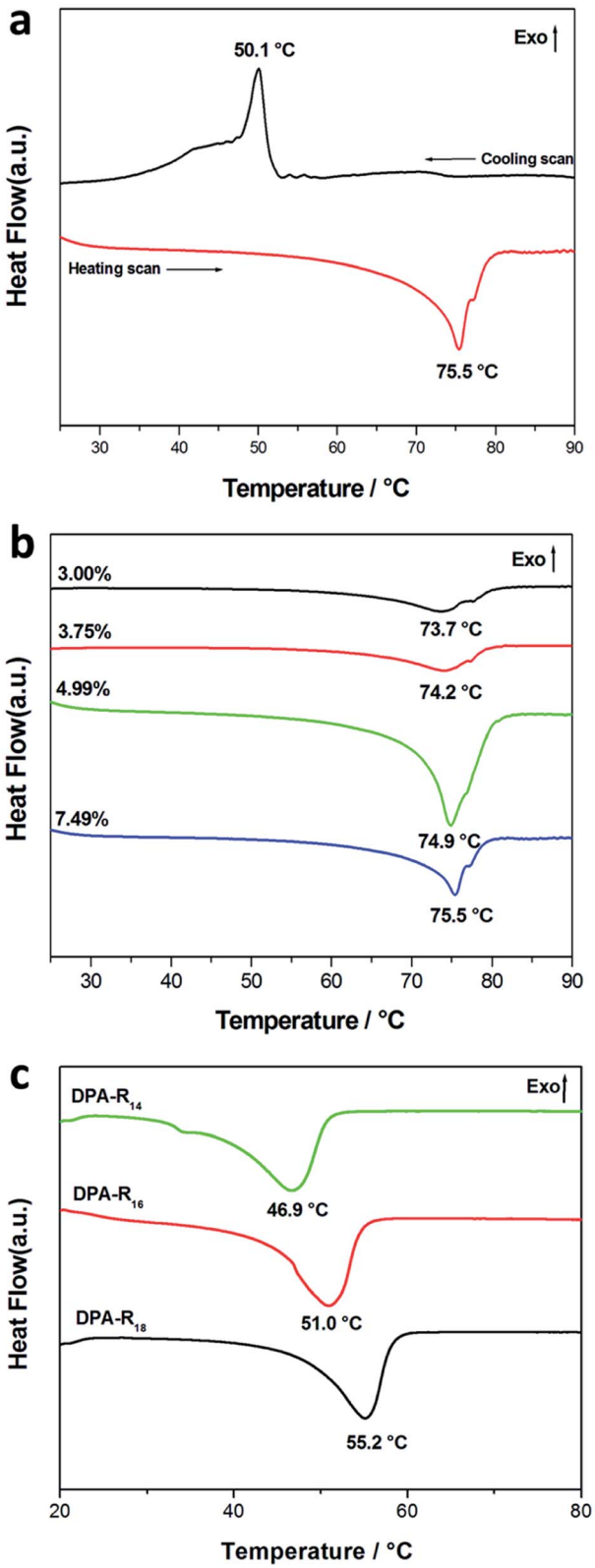

Fig. 2 DSC thermograms of the gels formed from (a) DPA-R_{18} in DMSO (7.49 wt%), (b) DPA-R_{18} in DMSO with different gelator concentrations (wt%) and (c) DPA-R_{14}, DPA-R_{16} and DPA-R_{18} in cyclohexane (3.75 wt%).

been found that none of the single component used in the experiment exhibits gelation ability in all tested solvents (Table S1–S3 in ESI†). However, part of the complexes formed from the selected dicarboxylic acid and R–NH_2 in molar ratio of 1/2 (denoted by ODA-R_n, IDA-R_n, PDA-R_n, TDA-R_n, TBA-R_n, TPA-R_n, DPA-R_n and EDA-R_n) display excellent gelation ability to organic liquids (Table 1 and S4–S10 in ESI†). Previous report[23] revealed that the complexes of stearic acid or eicosanoic acid and some of oligomeric amines exhibited excellent gelling ability to water. While in our experiments, no hydrogel could be formed from the complexes comprised of selected dicarboxylic acids and alkyl amines. These results imply that the gelling abilities of the complexes to organic liquids or water strongly depend on their molecular structures.

The supramolecular organogels obtained in the experiments are thermally reversible and stable at room temperature for more than 90 days. Upon heating, with increasing temperature over the critical transition temperature, the gels dissolve gradually and finally become clear solutions; while the solutions are cooled down to room temperature, gels are obtained again (Fig. 1). The result of gelation tests for DPA-R_n is summarized in Table 1. It can be found that DPA-R_{18} can gelatinize almost all organic liquids including strong and weak polar solvents, and most of the minimum gelator concentrations (MGCs) are very low, suggesting that the formation of "superorganogels". With the tail chain length of the alkyl amines shortening (from DPA-R_{18}, DPA-R_{16} to DPA-R_{14}), the kind of the organic liquids which can be gelatinized decreases. When the tail chain length of the alkyl amines is shorten to 12 (DPA-R_{12}), the complex cannot gelatinize any of organic liquids selected in the experiments.

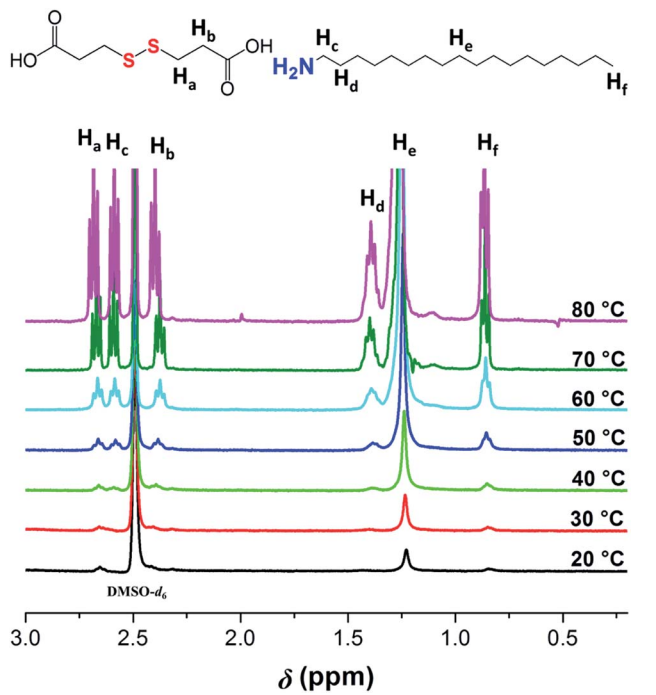

Fig. 3 Variable-temperature ^{1}H NMR spectra of the gel formed from DPA-R_{18} in DMSO-d_6.

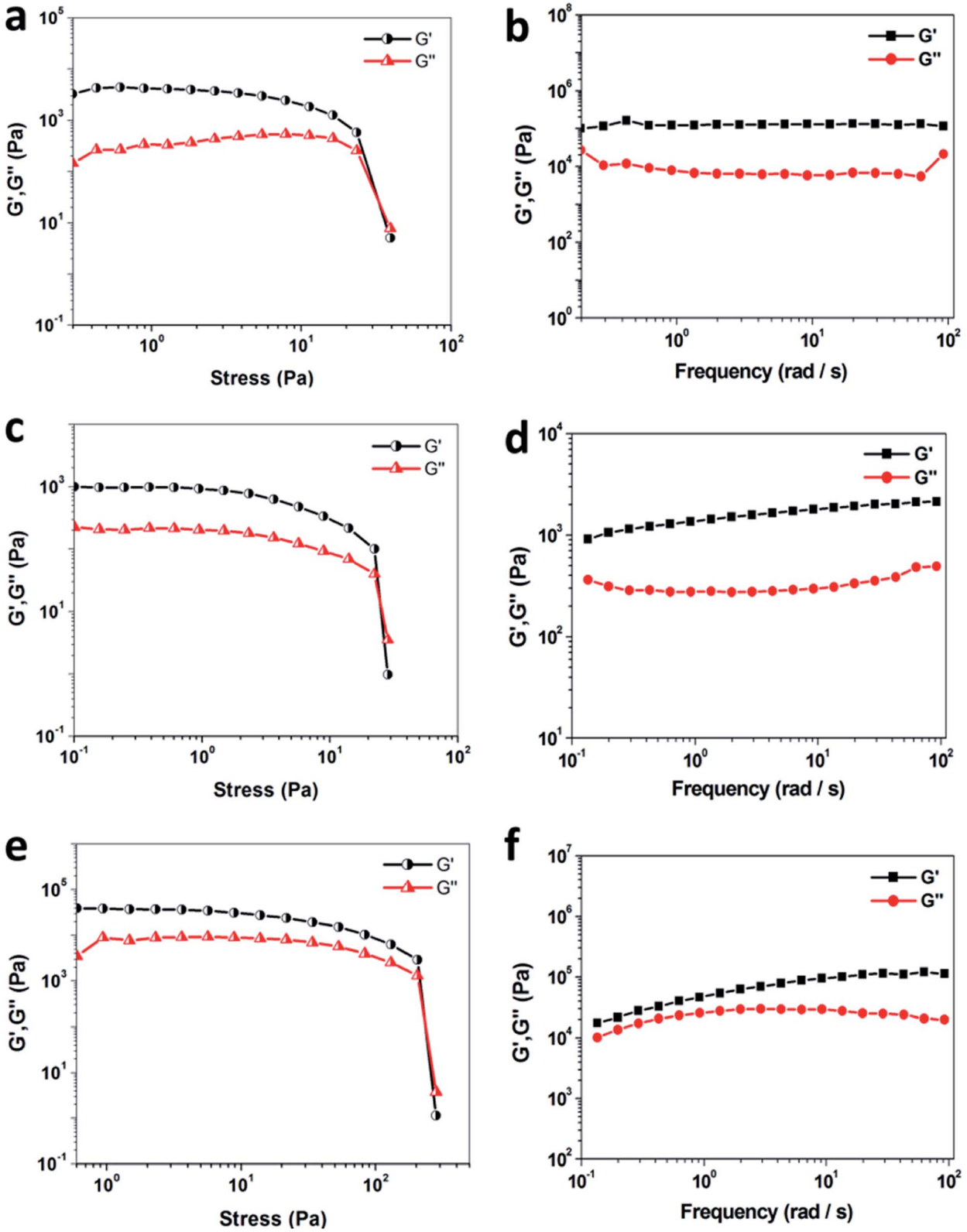

Fig. 4 Rheological behaviors of the organogels formed from DPA-R_{18} in DMF, chlorobenzene and isopropyl ether, respectively: (a, c and e) strain sweep results and (b, d and f) frequency sweep results at a constant strain of 5 Pa.

Moreover, the values of MGCs decrease as the tail chain length of gelators increases. For example, the MGCs of DPA-R_{14}, DPA-R_{16}, and DPA-R_{18} in DMSO are 2.55, 1.98 and 1.50 (wt%), respectively (Table 1). Similar results were also obtained from the gelation studies of the other gelators (PDA-R_n, TDA-R_n, TPA-R_n and EDA-R_n) in various organic mediums (Table S7–S10 in

ESI†). These results demonstrate that the primary alkyl amine with suitable length of tail chain is necessary for the formation of stable organogels. In addition, some of the complexes, such as TBA-R_n, ODA-R_n and IDA-R_n, present no gelatinizing ability in any of the tested organic liquids (Table S4–S6 in ESI†), indicating that the gelation abilities of the complexes to organic liquids also depend on their molecular structures of dicarboxylic acids. Therefore, the suitable length of alkyl chain and the structure of dicarboxylic acid in two-component gelators are very important for their gelation ability.

3.2 Morphology-controllable self-assembly

FE-SEM is a powerful tool to obtain the aggregate information of gelators in organo-/hydro-gels. In order to investigate the microstructure of organogels, the morphologies of various xerogels were observed by FE-SEM. Interestingly, the aggregate of DPA-R_{18} in tetrahydrofuran presented a rosette-like structure, which was fabricated with many flakes (thickness: ~200 nm) (Fig. 1a and b). However, bouquet-like structures were obtained from the organogels of DPA-R_{16} (Fig. 1c and d) and DPA-R_{14} (Fig. 1e and f) in tetrahydrofuran, indicating that the aggregation morphologies of gelators in organogels could be controlled by the tail chain length. Gelator molecules create complex three dimensional structures by entangling numerous flakes and entrapping abundant solvents in the interspace *via* surface tension and capillary forces, leading to the formation of organogels. Nano-flowers formed from some inorganics including SnO_2, ZnO, TiO_2, Fe_2O_3 and In_2O_3 have been reported previously,[24] but such rosette-like aggregates self-assembled by organic compounds are rare.[25]

Generally speaking, solvent properties play a key role in mediating the self-assembly of molecular.[26] As a consequence, the influence of solvent polarity on gel morphology was also explored. As shown in Fig. S1,† the aggregates of DPA-R_{18} in organogels prepared by different solvents display a variety of forms. In strong polar solvents, such as DMSO, methanol and ethanol, DPA-R_{18} self-assembles into fiber-like structure (Fig. S1 in ESI†). In medium polar solvents, such as THF, CH_2Cl_2, pyridine and $CHCl_3$, it self-assembles into flower-like structure (Fig. S2 in ESI†). In weakly polar solvents, such as cyclohexane and petroleum ether, the aggregates display sheet-shaped structure (Fig. S3 in ESI†). It clearly indicates that the morphologies of aggregates for the organogels could be regulated by solvent polarity.

3.3 Thermo-stability and thermo-reversibility

To gain further insights into the thermal stability of the as-prepared gels, DSC analyses were performed. Fig. 2a shows the DSC result of the gel formed from DPA-R_{18} in DMSO (7.49 wt%). It can be found that a peak at 75.5 °C corresponding to the transition from gel to sol is observed (heating scan) upon increasing temperature from 25 to 90 °C. When the sol is cooled, a peak at 50.1 °C correlated to the transition from sol to gel (cooling scan) is exhibited. Similar phenomena are also presented for the gels formed from DPA-R_{18} in cyclohexane and EDA-R_{18} in DMF (Fig. S4 in ESI†), indicating the thermo-reversible characteristics of the self-assembly process. Moreover, the melting temperatures (T_m) for gel–sol transition are higher than the forming temperatures (T_f) for sol–gel transition, which is the typical feature of many LMWGs-based gels.[27] Furthermore, the T_m is rising with increasing the gelator concentration (Fig. 2b). Similar results are also obtained from the DSC studies on the gel formed from DPA-R_{18} in cyclohexane and EDA-R_{18} in DMSO (Fig. S5 in ESI†), implying that the gelator concentration plays a significant role to the thermal stability of the gel. Fig. 2c illustrates the variation of T_m upon increasing the alkyl chain length of the gelator from 14 to 18 carbon atoms. With increasing the alkyl chain length, London dispersion forces in stabilizing the aggregates of organogels gradually increase, which is beneficial for gelation.[28] Therefore, an uptrend about the T_m is observed. Similar trends are also obtained from the DSC studies on the gel formed from EDA and amines in DMF (Fig. S6 in ESI†).

3.4 Variable-temperature ^{1}H NMR spectral studies

Generally, NMR techniques can provide some information in relation to the self-assembly process of the gelator in gel state. In most cases reported in previous literatures, the gelator's NMR signals completely disappear in gel state but present in liquid state.[29] Thus, temperature dependent ^{1}H NMR spectra of the gels formed separately from DPA-R_{18} and EDA-R_{18} in DMSO were recorded. As shown in Fig. 3 and S7,† the proton signals of the alkyl amine and dicarboxylic acid moieties have low sensitivity at 20 °C, which might be attributed to the long correlation time and slow tumbling rate in gel state, implying that there is a strong intermolecular aggregation of gelators.[30] By increasing temperature from 20 to 80 °C, the interaction between gelator and solvent molecules gradually increases, and the significantly-enhanced proton signals are also observed, indicating the gel–sol transformation. This

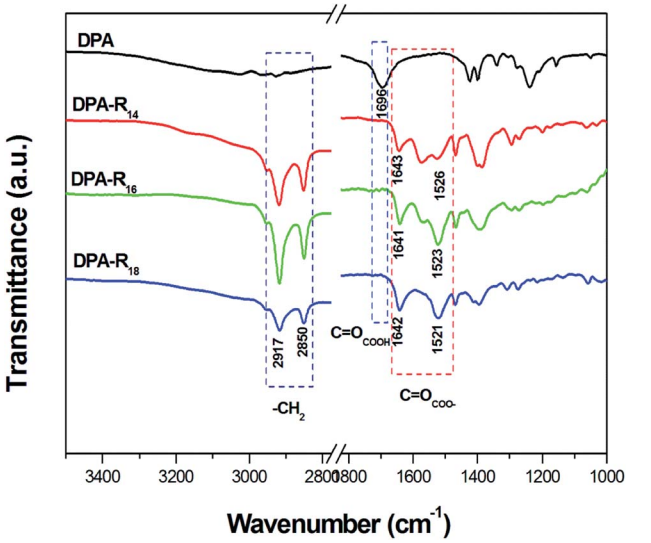

Fig. 5 FT-IR spectra of DPA and the xerogels formed from DPA-R_{14} (4.25 wt%), DPA-R_{16} (2.31 wt%) or DPA-R_{18} (1.67 wt%) in DMSO, respectively.

phenomenon illustrates a remarkable temperature dependent behavior and suggests that the gelatinous structure collapses at a higher temperature, which is in accordance with the results of the DSC analyses.

3.5 Mechanical properties

The mechanical property of a material is extremely important for its practical applications, so rheological measurements of organogels formed from DPA-R_{18} in various organic mediums (DMF, chlorobenzene and isopropyl ether) were performed. When the shear stress is over the critical shear stress, supramolecular organogels start to flow. As shown in Fig. 4a, c and e, the storage modulus (G') and loss modulus (G'') are independent of the stress below a critical strain region, and the deformation is always close to 0, implying that the gel structure keeps completely intact. When the stress is applied beyond a certain level, a catastrophic disruption of the gels occurs, as indicated by a steep drop in the values of both moduli and the reversal of the viscoelastic signal. Moreover, the frequency sweep analyses illustrate that both moduli exhibit less frequency dependence from 0.1–100 rad s^{-1} (Fig. 4b, d and f). All values of G' show an obvious elastic response, which are larger than that of G'' over the entire range of frequencies, indicating that these organogels formed in both strong polar (DMF) and medium polar (isopropyl ether) solvent are typical elastic materials.

Additionally, the rheological behaviors of organogels formed from DPA or EDA with various primary alkyl amines (R_{14}, R_{16}, and R_{18}) in DMSO were also studied. As exhibited in Fig. S8 and S9,† all values of G' decrease rapidly and fall below G'' after the shear stress is higher than the critical shear stress. The frequency sweep results show that both moduli exhibit less frequency dependence, and the value of G' gradually increases with increasing alkyl chain length from 14 to 18 carbon atoms,

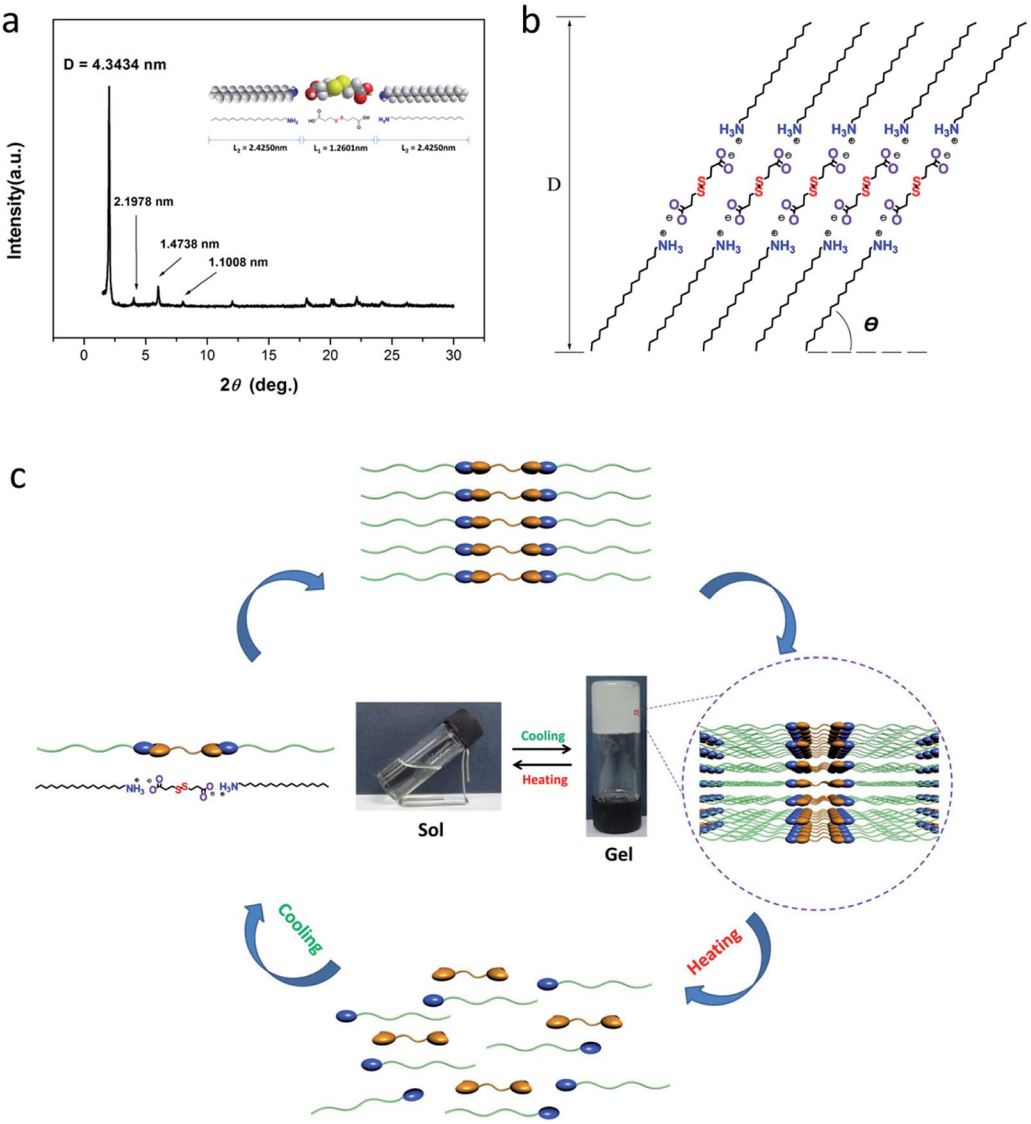

Fig. 6 (a) XRD pattern of DPA-R_{18} xerogel (7.49 wt%, solvent: DMSO; inset: CPK space-filling models of DPA and R_{18}–NH_2); (b) local microstructure of aggregates in DPA-R_{18} organogel; (c) schematic representation of self-assembly mechanism.

implying that the mechanical properties of the as-prepared organogels increase upon increasing alkyl chain length in gelators.

3.6 FT-IR spectral analysis

In order to further explore the gelation mechanism, FT-IR analyses were carried out. Commonly, supramolecular organogels are formed by van der Waals forces and hydrophobic interactions, *etc*.[7,9] The formation of salt between the dicarboxylic acid and the primary alkyl amine can be sensitively detected by FT-IR spectroscopy owing to the dicarboxylic acid has a characteristic stretching band of carbonyl in infrared region. Fig. 5 shows the FT-IR spectra of DPA and xerogels formed from DPA-R_{14}, DPA-R_{16} or DPA-R_{18} in DMSO, respectively. Compared with the spectrum of DPA, the strong peaks of the xerogels observed at 2917 and 2850 cm^{-1} could be ascribed to the stretching vibration of $-CH_2$ in the alkyl amine moiety. Moreover, the peak of the $C{=}O_{COOH}$ stretching vibration (1696 cm^{-1}) in the dicarboxylic acid moiety shifts to lower wavenumbers (1643, 1641 and 1642 cm^{-1}). Meanwhile, new absorption bands appear in the range of 1521–1526 cm^{-1}, indicating that all –COOH groups of DPA have been reacted with $R–NH_2$ by acid–base interaction.[23] Similar results are obtained in the gels formed in $CHCl_3$ and cyclohexane (Fig. S10 in ESI†). Additionally, the FT-IR spectra of the gels formed from EDA-R_{18}, EDA-R_{16} or EDA-R_{14} in DMSO/THF also demonstrate the formation of the corresponding salts (Fig. S11 in ESI†). Therefore, van der Waals forces and hydrophobic interactions are not the only mechanism for gelation, and acid–base interaction is also beneficial for the gel assembly.

3.7 X-ray diffraction studies

It has been established that the self-assembled structure of gelators in organogels can be well evaluated by that in xerogels or crystals, and much structural information could be obtained from the XRD spectrum.[31] In order to gain further insight into structures of self-assemblies, the XRD analyses of the xerogels formed from DPA-R_{18}, DPA-R_{16} or DPA-R_{14} in various organic solvents were performed. As displayed in Fig. 6a, periodic diffraction peaks (2θ = 2.03°, 4.08°, 6.11° and 8.13°) for the xerogel formed from DPA-R_{18} (7.49 wt%) in DMSO are observed in the small-angle region. Moreover, the corresponding *d*-spacings calculated by the Bragg equation are 4.3434, 2.1978, 1.4738 and 1.1008 nm, respectively, almost at a ratio of 1 : 1/2 : 1/3 : 1/4, indicating that the organogelator molecules self-assemble in a layered manner. Additionally, the long *d*-spacing (*D*) (4.3434 nm) is larger than the molecular length of $L_1 + L_2$ (3.6851 nm) evaluated *via* the Corey–Pauling–Koltun (CPK) space-filling model,[32] but smaller than that of $L_1 + 2L_2$ (6.1101 nm), implying that the aggregate unit consists of one deprotonated DPA molecule and two protonated alkyl amine moieties and self-assembles in a non-perpendicular manner. Based on literatures,[33] the calculated tilt angle is 45.3° (Fig. 6b). Similar results are also obtained for the gels formed in other organic solvents, such as THF, chlorobenzene, toluene, cyclohexane and $CHCl_3$ (Fig. S12 in ESI†).

Finally, the following self-assembly mechanism is proposed according to above analyses. As indicated in Fig. 6c, each deprotonated DPA molecule connects with two protonated alkyl amine moieties *via* electrostatic interactions, forming a one-dimensional (1D) chain structure. Subsequently, the 1D-chain is linked through van der Waals interactions to form a two-dimensional (2D) lamellar structure. These 2D-layers are further stacked with the adjacent layers, generating three-dimensional (3D) supramolecular structures. Organogelator molecules create complex 3D-networks by entangling numerous supramolecular structures and immobilize abundant organic liquid in the interspaces, resulting in the formation of supramolecular organogels.

4. Conclusions

In summary, a novel two-component supramolecular organogel system based on dicarboxylic acids and primary alkyl amines ($R–NH_2$) has been achieved in various organic media. The gelation ability is influenced by the alkyl chain length and the structure of dicarboxylic acid moieties in two-component gelators. The aggregation morphology of gelators could be efficiently adjusted by the solvent polarity and tail alkyl chain length. Interestingly, flower-like self-assemblies could be obtained in organic solvents with medium polarity, such as tetrahydrofuran, pyridine and dichloromethane, when the gelators possess a suitable length of carbon chain (R_{14}, R_{16} and R_{18}). Moreover, this kind of supramolecular organogel system with controllable self-assembled structures displays excellent thermo-reversibility and mechanical properties. In addition, the intermolecular acid–base interaction and van der Waals interaction are critical driving forces in the process of gelation. This work can provide a novel strategy for constructing the tunable supramolecular nano-architectures with potential applications in functional soft materials.

Conflicts of interest

There are no conflicts of interest to declare.

Acknowledgements

This work was financially supported by the National Natural Science Foundation of China (21663004, 21661020 and 21961021), Major Project for Science and Technology of Jiangxi Province (20152ACB21016), Natural Science Foundation of Jiangxi Province (2014ACB20009), Science and Technology Project of Jiangxi Provincial Department of Education (GJJ190774) and Graduate Innovation Foundation of Nanchang University (cx2016012).

References

1 (*a*) R. Kuosmanen, K. Rissanen and E. Sievänen, *Chem. Soc. Rev.*, 2020, **49**, 1977–1998; (*b*) M. Chetia, S. Debnath, S. Chowdhury and S. Chatterjee, *RSC Adv.*, 2020, **10**, 5220–5233; (*c*) G. Qi, Y. Gao, L. Wang and H. Wang, *Adv. Mater.*,

2018, **30**, 1703444; (*d*) S. Onogi, H. Shigemitsu, T. Yoshii, T. Tanida, M. Ikeda, R. Kubota and I. Hamachi, *Nat. Chem.*, 2016, **8**, 743–752.
2 H. Cao, P. Duan, X. Zhu, J. Jiang and M. Liu, *Chem.–Eur. J.*, 2012, **18**, 5546–5550.
3 J. Zhong, H. Fu, X. Jia, H. Lou, T. Wan, H. Luo, H. Liu, D. Zhong and X. Luo, *RSC Adv.*, 2019, **9**, 11824–11832.
4 T. Bollhorst, K. Rezwan and M. Maas, *Chem. Soc. Rev.*, 2017, **46**, 2091–2126.
5 L. Qin, L. Zhang, Q. Jin, J. Zhang, B. Han and M. Liu, *Angew. Chem., Int. Ed.*, 2013, **52**, 1–6.
6 (*a*) F. Wang and C. Feng, *Angew. Chem., Int. Ed.*, 2018, **57**, 5655–5659; (*b*) G. Liu, J. Liu, C. Feng and Y. Zhao, *Chem. Sci.*, 2017, **8**, 1769–1775; (*c*) M. Liu, L. Zhang and T. Wang, *Chem. Rev.*, 2015, **115**, 7304–7397.
7 S. S. Babu, V. K. Praveen and A. Ajayaghosh, *Chem. Rev.*, 2014, **114**, 1973–2129.
8 (*a*) T. Shimizu, W. Ding and N. Kameta, *Chem. Rev.*, 2020, **120**, 2347–2407; (*b*) B. An, J. Gierschner and S. Y. Park, *Acc. Chem. Res.*, 2012, **45**, 544–554; (*c*) P. Dastidar, *Chem. Soc. Rev.*, 2008, **37**, 2699–2715.
9 B. O. Okesola and D. K. Smith, *Chem. Soc. Rev.*, 2016, **45**, 4226–4251.
10 (*a*) A. M. Vibhute, V. Muvvala and K. M. Sureshan, *Angew. Chem., Int. Ed.*, 2016, **55**, 7782–7785; (*b*) A. Prathap and K. M. Sureshan, *Chem. Commun.*, 2012, **48**, 5250–5252.
11 Q. Lin, T. Lu, X. Zhu, T. Wei, H. Li and Y. Zhang, *Chem. Sci.*, 2016, **7**, 5341–5346.
12 (*a*) Z. Feng, T. Zhang, H. Wang and B. Xu, *Chem. Soc. Rev.*, 2017, **46**, 6470–6479; (*b*) B. Escuder, F. Rodríguez-Llansola and J. F. Miravet, *New J. Chem.*, 2010, **34**, 1044–1054.
13 Y. Zhang, T. Luan, Q. Cheng, W. An, R. Tang, P. Xing and A. Hao, *Langmuir*, 2019, **35**, 4133–4139.
14 X. Zhu, Y. Li, P. Duan and M. Liu, *Chem.–Eur. J.*, 2010, **16**, 8034–8040.
15 L. Zhang, C. Liu, Q. Jin, X. Zhua and M. Liu, *Soft Matter*, 2013, **9**, 7966–7973.
16 S. Lee, S. Oh, J. Lee, Y. Malpani, Y. Jung, B. Kang, J. Lee, K. Ozasa, T. Isoshima, S. Lee, M. Hara, D. Hashizume and J. Kim, *Langmuir*, 2013, **29**, 5869–5877.
17 B. Bag and S. S. Dash, *Langmuir*, 2015, **31**, 13664–13672.
18 (*a*) P. Xing and Y. Zhao, *Acc. Chem. Res.*, 2018, **51**, 2324–2334; (*b*) J. Raeburn and D. J. Adams, *Chem. Commun.*, 2015, **51**, 5170–5180; (*c*) V. M. P. Vieira, L. L. Haya and D. K. Smith, *Chem. Sci.*, 2017, **8**, 6981–6990; (*d*) P. R. A. Chivers and D. K. Smith, *Nat. Rev. Mater.*, 2019, **4**, 463–478; (*e*) D. J. Cornwell, O. J. Daubney and D. K. Smith, *J. Am. Chem. Soc.*, 2015, **137**, 15486–15492.
19 W. Edwards and D. K. Smith, *J. Am. Chem. Soc.*, 2013, **135**, 5911–5920.
20 J. Liu, J. Li, P. Lin, N. Zhang, X. Han, B. Zhang and J. Song, *Chem. Commun.*, 2016, **52**, 13975–13978.
21 K. Fan, H. Kong, X. Wang, X. Yang and J. Song, *RSC Adv.*, 2016, **6**, 80934–80938.
22 D. Zhong, L. Liao, K. Wang, H. Liu and X. Luo, *Soft Matter*, 2015, **11**, 6386–6392.
23 H. Basit, A. Pal, S. Sen and S. Bhattacharya, *Chem.–Eur. J.*, 2008, **14**, 6534–6545.
24 (*a*) C. Xu, P. R. Anusuyadevi, C. Aymonier, R. Luque and S. Marre, *Chem. Soc. Rev.*, 2019, **48**, 3868–3902; (*b*) H. Wang and A. L. Rogach, *Chem. Mater.*, 2014, **26**, 123–133; (*c*) L. Sang, Y. Zhao and C. Burda, *Chem. Rev.*, 2014, **114**, 9283–9318; (*d*) H. Zhang, R. Wu, Z. Chen, G. Liu, Z. Zhang and Z. Jiao, *CrystEngComm*, 2012, **14**, 1775–1782.
25 (*a*) M. Salimimarand, D. D. La, M. A. Kobaisi and S. V. Bhosale, *Sci. Rep.*, 2017, **7**, 42898; (*b*) X. Zhou, Q. Jin, L. Zhang, Z. Shen, L. Jiang and M. Liu, *Small*, 2016, **12**, 4743–4752; (*c*) R. D. Mukhopadhyay, V. K. Praveen, A. Hazra, T. K. Majic and A. Ajayaghosh, *Chem. Sci.*, 2015, **6**, 6583–6591.
26 (*a*) Z. Quan, H. Xu, C. Wang, X. Wen, Y. Wang, J. Zhu, R. Li, C. J. Sheehan, Z. Wang, D. M. Smilgies, Z. Luo and J. Fang, *J. Am. Chem. Soc.*, 2014, **136**, 1352–1359; (*b*) Z. Ding, R. Xing, Y. Sun, L. Zheng, X. Wang, J. Ding, L. Wang and Y. Han, *RSC Adv.*, 2013, **3**, 8037–8046; (*c*) W. Edwards, C. A. Lagadec and D. K. Smith, *Soft Matter*, 2011, **7**, 110–117; (*d*) P. Jonkheijm, P. van der Schoot, A. P. H. J. Schenning and E. W. Meijer, *Science*, 2006, **313**, 80–83.
27 (*a*) A. Pal, Y. K. Ghosh and S. Bhattacharya, *Tetrahedron*, 2007, **63**, 7334–7348; (*b*) M. Moniruzzaman and P. R. Sundararajan, *Langmuir*, 2005, **21**, 3802–3807.
28 (*a*) M. A. Rogersa and R. G. Weiss, *New J. Chem.*, 2015, **39**, 785–799; (*b*) M. George and R. G. Weiss, *Acc. Chem. Res.*, 2006, **39**, 489–497.
29 (*a*) G. Yu, X. Yan, C. Han and F. Huang, *Chem. Soc. Rev.*, 2013, **42**, 6697–6722; (*b*) F. Allix, P. Curcio, Q. N. Pham, G. Pickaert and B. Jamart-Grégoire, *Langmuir*, 2010, **26**, 16818–16827.
30 (*a*) X. Jia, J. Wang, D. Zhong, J. Wu, B. Zhao, D. den Engelsen and X. Z. Luo, *RSC Adv.*, 2016, **6**, 109425–109433; (*b*) S. Yagai, M. Higashi, T. Karatsu and A. Kitamura, *Chem. Mater.*, 2004, **16**, 3582–3585.
31 E. R. Draper and D. J. Adams, *Chem. Soc. Rev.*, 2018, **47**, 3395–3405.
32 (*a*) X. Luo, Z. Li, W. Xiao, Q. Wang and J. Zhong, *J. Colloid Interface Sci.*, 2009, **336**, 803–807; (*b*) D. J. Cram, *Science*, 1988, **240**, 760–767.
33 (*a*) X. Luo, Z. Zhang and Y. Liang, *Langmuir*, 1994, **10**, 3213–3216; (*b*) J. Umermura, T. Kamata, T. Kawai and T. Takenaka, *J. Phys. Chem.*, 1990, **94**, 62–67.

